

Direct laser writing for nanoporous liquid core laser sensors

Tobias Grossmann,^{1,2,*} Mads Brøkner Christiansen,³ Jeffrey Peterson,³ Heinz Kalt,¹ Timo Mappes,² and Anders Kristensen³

¹Institute of Applied Physics and DFG Center for Functional Nanostructures CFN, Karlsruhe Institute of Technology KIT, 76128 Karlsruhe, Germany

²Institute of Microstructure Technology, Karlsruhe Institute of Technology, 76128 Karlsruhe, Germany

³Department of Micro- and Nanotechnology, DTU Nanotech, Technical University of Denmark, Kgs. Lyngby, 2800, Denmark

*tobias.grossmann@kit.edu

Abstract: We report the fabrication of nanoporous liquid core lasers via direct laser writing based on two-photon absorption in combination with thiolene-chemistry. As gain medium Rhodamine 6G was embedded in the nanoporous polybutadiene matrix. The lasing devices with thresholds of 19 $\mu\text{J}/\text{mm}^2$ were measured to have bulk refractive index sensitivities of 169 nm/RIU at a laser wavelength of 600 nm, demonstrating strongly increased overlap of the modes with the analyte in comparison to solid state evanescent wave sensors.

©2012 Optical Society of America

OCIS codes: (140.2050) Dye lasers; (140.3948) Microcavity devices; (140.7300) Visible lasers; (160.5470) Polymers; (220.4241) Nanostructure fabrication.

References and links

1. D. Erickson, D. Sinton, and D. Psaltis, "Optofluidics for energy applications," *Nat. Photonics* **5**(10), 583–590 (2011).
2. H. Schmidt and A. R. Hawkins, "The photonic integration of non-solid media using optofluidics," *Nat. Photonics* **5**(10), 598–604 (2011).
3. X. Fan and I. M. White, "Optofluidic microsystems for chemical and biological analysis," *Nat. Photonics* **5**(10), 591–597 (2011).
4. M. Mancuso, J. M. Goddard, and D. Erickson, "Nanoporous polymer ring resonators for biosensing," *Opt. Express* **20**(1), 245–255 (2012).
5. H. Schmidt and A. R. Hawkins, "Optofluidic waveguides: I. Concepts and implementations," *Microfluid. Nanofluid.* **4**(1-2), 3–16 (2008).
6. T. Dallas and P. K. Dasgupta, "Light at the end of the tunnel: recent analytical applications of liquid-core waveguides," *TRAC-Trend. Anal. Chem.* **23**, 385–392 (2004).
7. H. Li and X. Fan, "Characterization of sensing capability of optofluidic ring resonator biosensors," *Appl. Phys. Lett.* **97**(1), 011105 (2010).
8. L. He, S. K. Ozdemir, J. Zhu, W. Kim, and L. Yang, "Detecting single viruses and nanoparticles using whispering gallery microlasers," *Nat. Nanotechnol.* **6**(7), 428–432 (2011).
9. Y. Sun and X. Fan, "Distinguishing DNA by analog-to-digital-like conversion by using optofluidic lasers," *Angew. Chem.* **124**(5), 1262–1265 (2012).
10. A. M. Armani, D. K. Armani, B. Min, K. J. Vahala, and S. M. Spillane, "Ultra-high-Q microcavity operation in H_2O and D_2O ," *Appl. Phys. Lett.* **87**(15), 151118 (2005).
11. N. Gopalakrishnan, K. S. Sagar, M. B. Christiansen, M. E. Vigild, S. Ndoni, and A. Kristensen, "UV patterned nanoporous solid-liquid core waveguides," *Opt. Express* **18**(12), 12903–12908 (2010).
12. K. Sagar, N. Gopalakrishnan, M. B. Christiansen, A. Kristensen, and S. Ndoni, "Photolithographic fabrication of solid-liquid core waveguides by thiol-ene chemistry," *J. Micromech. Microeng.* **21**(9), 095001 (2011).
13. N. Gopalakrishnan, M. B. Christiansen, and A. Kristensen, "Nanofiltering via integrated liquid core waveguides," *Opt. Lett.* **36**(17), 3350–3352 (2011).
14. G. von Freymann, A. Ledermann, M. Thiel, I. Staude, S. Essig, K. Busch, and M. Wegener, "Three-dimensional nanostructures for photonics," *Adv. Funct. Mater.* **20**(7), 1038–1052 (2010).
15. L. Schulte, A. Grydgaard, M. R. Jakobsen, P. P. Szczykowski, F. Guo, M. E. Vigild, R. H. Berg, and S. Ndoni, "Nanoporous materials from stable and metastable structures of 1,2-PB-b-PDMS block copolymers," *Polymer (Guildf.)* **52**(2), 422–429 (2011).
16. I. M. White and X. Fan, "On the performance quantification of resonant refractive index sensors," *Opt. Express* **16**(2), 1020–1028 (2008).

1. Introduction

Over the last years, optofluidic devices have emerged as highly promising building blocks for a multitude of technologies where simultaneous and precise control of light and fluids on a nano- and microscale is essential, such as energy conversion [1], on-chip photonics [2] and chemical and biological sensing platforms [3,4]. In order to achieve highly integrated optofluidic circuits, fluidic channels can be used to guide light and liquid through the same physical volume known as liquid-core waveguides (LCWs) [5,6]. This type of waveguide enables large light-matter interaction lengths in combination with small detection volumes, making it an inherently suitable platform for biological/chemical detection. Especially when LCWs form a resonant microcavity with high quality factors (Q factors) such as whispering gallery mode (WGM) microresonators, low detection limits can be achieved [3,7]. Besides using passive microcavities as transducers, WGM microcavity lasers have emerged as an attractive alternative to their passive counterparts due to potentially narrower linewidths and the possibility to use free-space excitation and detection schemes. Active microcavities have been used for the detection of single nanoparticles [8] or DNA [9]. The use of organic gain materials, such as dyes, enable the detection in the visible spectral region, where cavity losses due to absorption of aqueous solutions become negligible [10]. In order to achieve low detection limits due to the small probing wavelength in comparison to infra-red wavelengths, a large overlap of the optical modes with the analyte in addition to a high Q factor is necessary, making WGM lasers based on LCWs attractive for intra-cavity sensing.

A promising approach for the realization of LCWs is based on nanoporous polymers (NP) [11,12], where the waveguide core is a hydrophilic NP infiltrated by a liquid and the cladding is formed by a hydrophobic NP without liquid. Therefore the core is a solid-liquid 'alloy'. These waveguides are termed solid-liquid core waveguides (SLCWs). The refractive index contrast between core and cladding in this configuration is around 0.16 RIU [12]. SLCWs are therefore suitable for the fabrication of optofluidic microcavities. In previous work, these SLCWs were fabricated by standard UV photolithography with a quartz chromium mask and thiolene-chemistry [12]. While first devices fabricated by this process could be successfully used as waveguides with nanofiltering effect [13], technical drawbacks of this planar fabrication technique had to be faced, such as a limited lateral resolution ($\sim 1 \mu\text{m}$) and no control of the exposure profile normal to the substrate, inherently rendering the waveguides multi-mode.

In this work, we demonstrate how direct laser writing (DLW) based on two-photon absorption (TPA) in combination with thiolene-chemistry can be used to define hydrophilic regions within nanoporous polybutadiene, which allows for three-dimensional control of the SLCW geometry and in principle lateral feature sizes of several hundred nanometers [14]. We realize nanoporous liquid core ring resonator lasers by doping the NP with Rhodamine 6G, resulting in lasing thresholds around $19 \mu\text{J}/\text{mm}^2$ and determine spectrometer-limited laser linewidths of 70 pm. The lasing devices were measured to have bulk refractive index sensitivities of 169 nm/RIU at a laser wavelength of 600 nm, demonstrating these ring resonators based on nanoporous liquid core waveguides to have an increased light matter interaction compared to solid state WGM sensors where only the evanescent field probes the liquid analyte in the surrounding.

2. Fabrication of nanoporous dye lasers by direct laser writing

In the following, the fabrication of the nanoporous ring resonator lasers is described before we turn to the lasing properties.

The fabrication process of ring resonator lasers is carried out in three steps: (1) fabrication of nanoporous 1,2-polybutadiene polymer films, (2) exposure of a ring in the NP by two photon absorption, and (3) doping of the polymer matrix with laser dye. Details about the preparation of nanoporous 1,2-polybutadiene polymer films have been described in previous

work [12,15] and are only mentioned here briefly. First, the di-block copolymer 1,2-polybutadiene-*b*-polydimethylsiloxane (1,2-PB-*b*-PDMS) is dissolved in tetrahydrofuran (THF). The thermal cross-linking agent dicumyl peroxide is added and the solution is casted onto a silicon wafer coated with a fluorinated organosilane layer (tridecafluoro-(1,1,2,2)-tetrahydrooctyl-trichlorosilane) in order to avoid adhesion of the polymer to the wafer surface. The casted film is dried and sandwiched by a second silicon wafer with 50 μm high ridges serving as stress relief pattern during the cross-linking in an EVG 520 hot embosser with an applied pressure of 255 kPa at 145°C for 90 min. After separation from the casting form, the 50 μm thick substrates are used for further processing. The cross-linked polymer substrates are subjected to selective chemical etching of the PDMS block using tetrabutylammonium fluoride in THF for 24 h. The substrates are further washed sequentially in THF and ethanol. The remaining 1,2 polybutadiene polymer contains a self assembled network of 14 nm diameter pores with a porosity of 44% [15].

In order to hydrophilize the hydrophobic NP, photo-grafting of thiol compounds containing hydrophilic groups onto the inner surfaces of the nanopores was applied. In contrast to previous work [12] this process was not performed with standard UV photolithography but with two photon absorption. 2-Benzyl-2-(dimethylamino)-4'-morpholinobutyrophenone was used as a photoinitiator (PI), which initiates the reaction of mercaptosuccinic acid (MSA) onto the surface of the nanopores. MSA is a hydrophilic molecule with two terminal carboxylic groups along with a thiol group. MSA (500mM) and the PI (10mM) were dissolved in ethanol. The nanoporous polymer was immersed in the thiol solution for 30 min before the exposure to facilitate loading of solution into the nanopores and stays immersed in the thiol solution during the exposure.

A commercial DLW system (Photonic Professional, Nanoscribe, Karlsruhe, Germany), exposing with a frequency-doubled, pulsed fiberlaser (pulse length below 150 fs, repetition

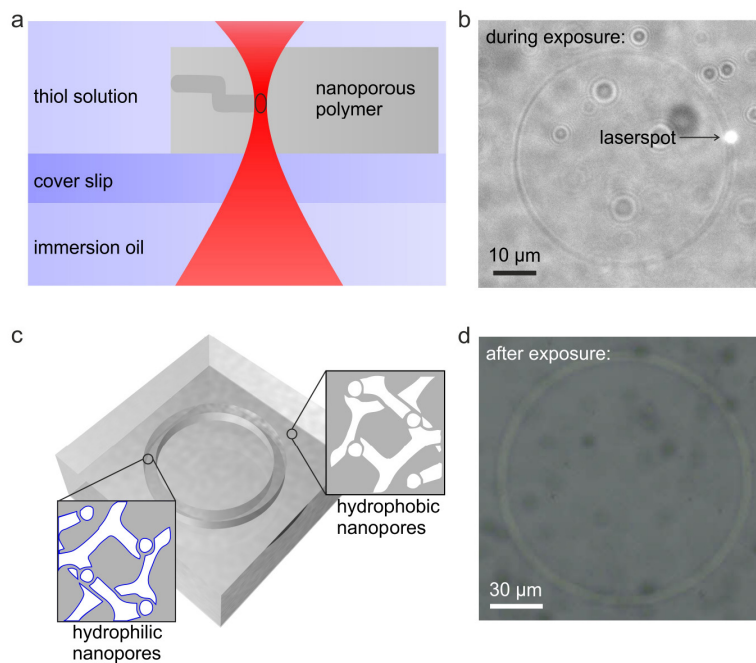


Fig. 1. (a) Schematic of the layer system used for fabrication of nanoporous ring resonator lasers via DLW. (b) Optical micrograph during the exposure showing the laserspot and the exposed ring. (c) Schematic of the sample after the exposure. The exposed areas contain hydrophilic nanopores and are embedded within the hydrophobic nanoporous polymer. (d) Optical micrograph of the sample after the direct laser writing process. The ring has a diameter of 150 μm and a width of 5 μm .

rate 100 MHz at 780 nm wavelength) was used. The laser beam was focused into the sample by an immersion oil objective (numerical aperture NA = 1.4, 100x). A schematic of the layer system used for the exposure is depicted in Fig. 1(a). The laser beam passes the immersion oil and the cover slip before it is focused into the transparent polymer sample. The size of the ellipsoidal volume pixel (voxel) in which the TPA occurs was 1 μm in the propagation direction of the beam and several hundred micrometers in the lateral direction. During the exposure, the modification of the nanoporous polymer is easily visible by a refractive index change of the material due to the formation of hydrophilic end-groups in the nanopores. Figure 1(b) shows an image during the exposure of a ring, where the laserspot and the exposed ring can be seen. After the exposure, the sample was washed in ethanol to completely remove the thiol solution and dried afterwards. The exposed rings with hydrophilic nanopores were embedded within the hydrophobic nanoporous polymer as depicted schematically in Fig. 1(c). Figure 1(d) shows a microscope image of an exposed ring with a diameter of 150 μm and a width of 5 μm after the exposure. The thickness of the exposed ring is around 10 μm and was written by stacking 10 layers each with a thickness of 1 μm , which was defined by the voxel size.

The gain material was integrated after the lithographic definition of the resonator. This was achieved by doping the entire polymer matrix with the laser dye Rhodamine 6G (rh6G) as depicted schematically in Fig. 2(a). The substrate was submerged for 24 h in a saturated solution of rh6G dissolved in THF. The solvent causes the polymer matrix to swell, enabling diffusion of dye into the matrix. The density of dye molecules is strongly increased in the nanopores with hydrophilic end-groups as can be seen in the microscope image depicted in Fig. 2(b), due to binding of the relatively polar rh6G molecules onto the surface of the nanopores. In order to guide light in the liquid core resonator, the exposed ring has to be infiltrated with water. A waterfilm on top of the substrate is already sufficient to cause condensation of evaporated water within the ring and to infiltrate the hydrophilic nanopores (see Fig. 2(c)). The infiltrated region has a refractive index of 1.42, which is about 0.16 RIU higher than the hydrophobic regions without water and thus sufficient to guide light [13]. Figure 2(d) shows a microscope image of an exposed ring with a water film on top of the

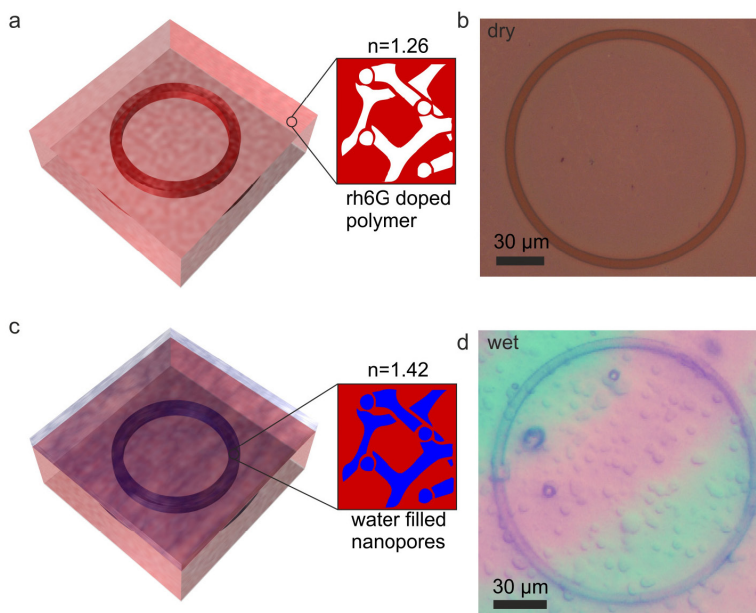


Fig. 2. (a) Schematic and (b) microscope image of a dye-doped nanoporous sample without water. (c) Schematic and (d) microscope image of a sample with a waterfilm on top resulting in an infiltrated ring with increased refractive index compared to the surrounding polymer matrix.

sample. In this case the sample was undoped and the contrast between exposed ring and unexposed surrounding was increased due to uptake of water within the ring. This can be clearly seen by comparison with a dry sample depicted in Fig. 1(d). The interference effect in Fig. 2(d) is due to a thin air film between the transparent sample and the stage it was layed upon.

3. Lasing properties of nanoporous liquid core dye lasers

To characterize the lasing properties, the dye-doped samples were infiltrated with water and optically pumped from above with 8 ns pulses of a frequency doubled Nd:YAG laser at a pump wavelength of 532 nm and a repetition rate of 10 Hz. Output emission was collected either at the edge of the chip with a multimode optical fiber, or perpendicularly to the sample with a microscope objective ($NA = 0.4$, 20x) and analyzed in a spectrometer. Spectra of the laser output for increasing pump fluence are depicted in Fig. 3(a). Above a pump fluence of $12 \mu\text{J}/\text{mm}^2$ several sharp lasing modes appear in the spectrum due to amplification of WGMs by the dye. Output intensity as function of increasing excitation pump fluence is exemplarily shown in Fig. 3(b) for the grey marked mode in Fig. 3(a). The input-output curve has a kink at a threshold pump fluence of $19 \mu\text{J}/\text{mm}^2$, determining the onset of lasing for this particular mode. The value of the threshold inferred from the intercept of the two linear regimes is the best possible upper estimation in this case. This takes into account both fluorescence backgrounds, the one from the ring resonator itself as well as the other one from the surrounding doped polymer. The inset of Fig. 3(b) shows a microscope image of the ring laser with a diameter of $150 \mu\text{m}$ under optical excitation, where the excitation wavelength is filtered out. Above threshold equally spaced laser modes were observed as shown with higher

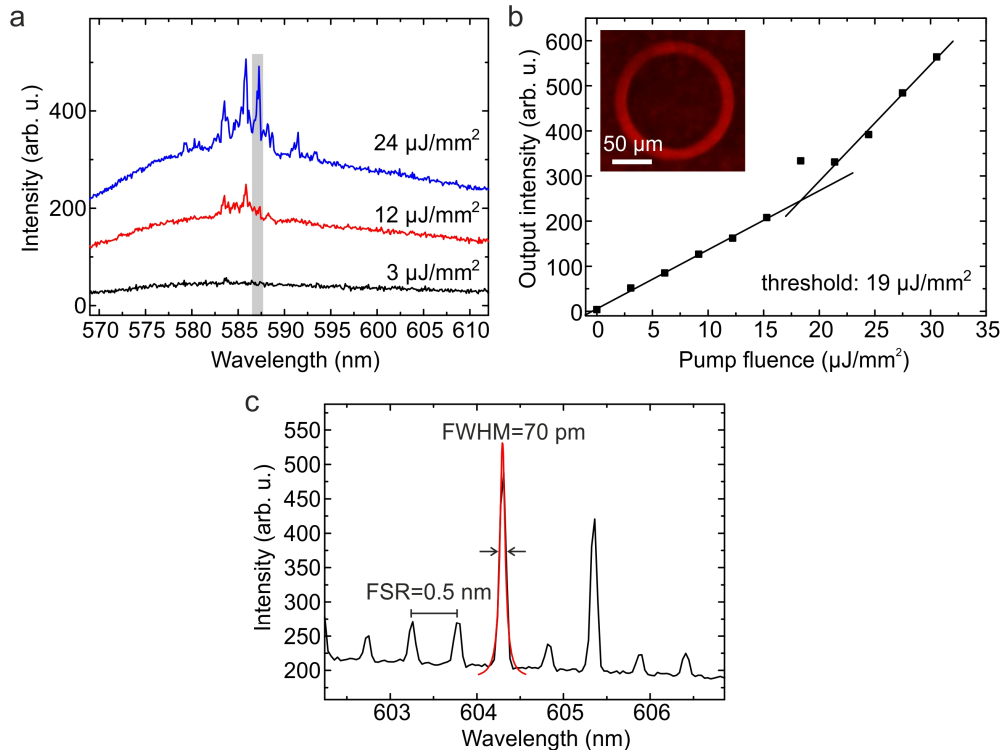


Fig. 3. (a) Output spectrum of an optically pumped dye-doped liquid core ring resonator laser for different pump fluences. (b) Input-output curve of the grey marked mode in (a) at 587 nm with a threshold pump fluence of $19 \mu\text{J}/\text{mm}^2$. (c) High-resolution spectrum above lasing threshold, showing multiple laser modes between 603 nm and 606 nm with linewidths of 70 pm and a free spectral range of 0.5 nm.

resolution in Fig. 3(c). The free spectral range $\Delta\lambda_{\text{FSR}}$ measured in the spectrum was 0.5 nm, which is in agreement with the value expected from the equation $\Delta\lambda_{\text{FSR}} = \lambda^2 / (2\pi n R) = 0.54 \text{ nm}$, with a refractive index of $n=1.42$, a radius of $R = 75 \mu\text{m}$, and a wavelength of $\lambda = 600 \text{ nm}$. The linewidth of the laser modes was measured to be 70 pm and limited by the spectrometer resolution using a grating with 1200 lines/mm.

To investigate the sensitivity of a liquid core WGM laser upon change of the surrounding refractive index, tuning of the lasing modes was performed by changing the liquid core's refractive index with water containing different glucose concentrations. The shifts of the laser modes due to refractive index changes is a direct measure of the sensitivity, which is often referred to as bulk refractive index sensitivity (BRIS), an often used quantity to compare different types of sensors. The BRIS mainly depends on the fraction of optical intensity of a mode interacting with the liquid analyte [16], which is thus expected to be strongly increased in liquid core microcavities. The response of the nanoporous liquid core laser with a radius of 75 μm to changing refractive index surroundings was measured by infiltrating the sample with different concentrations of glucose dissolved in water and taking a laser spectrum for every concentration. The shift (in comparison to pure water) of a single laser mode is depicted in Fig. 4. Exemplarily, the lasing spectra for the solutions with the three lowest refractive indices are shown in the inset of Fig. 4. The slope of the linear fit was measured to be 169 nm/RIU. This value is around one order of magnitude larger than in solid state WGM microcavities with comparable radius and wavelength [17] and demonstrates the high potential of liquid core resonators for sensing applications due to the strongly increased overlap of the modes with the analyte in comparison to evanescent wave sensors. With a sensitivity of 169 nm/RIU the detection limit of the nanoporous liquid core laser was determined to be 3×10^{-5} RIU, given that the smallest detectable laser line shift (3σ) is 6 pm.

Another interesting property of the present platform is the huge inner surface area of the NP of $283 \pm 14 \text{ m}^2/\text{g}$ [12]. This would provide an inherently large sensitivity to surface refractive index changes, if the inner pore surfaces were modified to bind specific analytes.

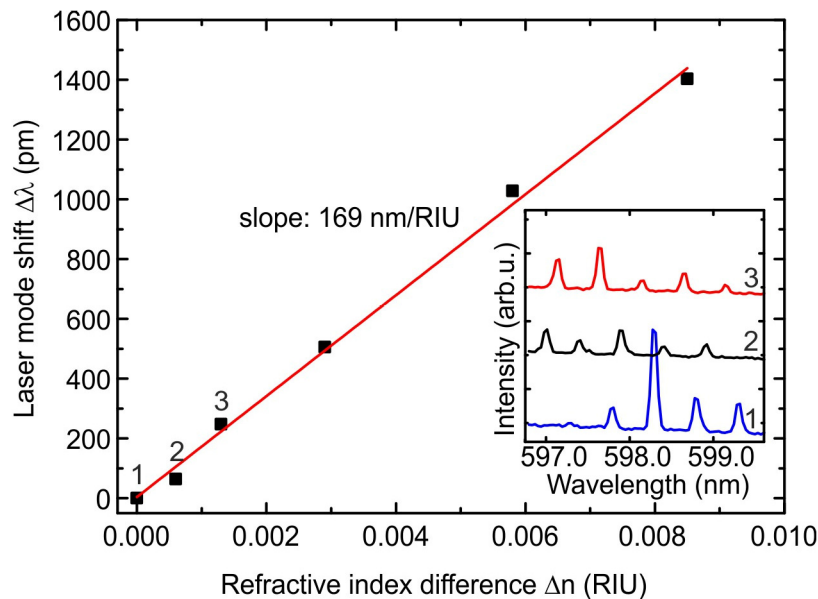


Fig. 4. Shift of the laser mode for changing refractive index surrounding for different glucose concentrations compared to pure water. The inset exemplarily shows the lasing spectra for the solutions with the three lowest concentrations. The depicted laser modes shift by 169 nm/RIU. Varying relative intensities between the peaks are related to a shift of the gain spectrum due to bleaching of dye molecules during laser operation.

4. Conclusion

In summary, we have applied direct laser writing (DLW) in combination with thiolene-chemistry to define hydrophilic regions within a nanoporous polymer which can then be infiltrated with water and thus forms a liquid core waveguide. Nanoporous liquid core ring resonator lasers were fabricated by doping the polymer matrix with dye. Thus the liquid applied to these devices did not require any treatment or admixing to serve as liquid core of the cavity. The liquid core lasing devices were measured to have bulk refractive index sensitivities of 169 nm/RIU at a wavelength of 600 nm, which is an order of magnitude larger sensitivity than in comparable solid state WGM sensors, demonstrating the large light matter interaction in these active intra-cavity sensing devices.

Acknowledgments

This work has been supported by the DFG Research Center for Functional Nanostructures (CFN) Karlsruhe, by a grant from the Ministry of Science, Research, and the Arts of Baden-Württemberg (Grant No. Az:7713.14-300) and by the German Federal Ministry for Education and Research BMBF (Grant No. FKZ 13N8168A). T. M.'s Young Investigator Group (YIG 08) received financial support from the Concept for the Future of the Karlsruhe Institute of Technology (KIT) within the framework of the German Excellence Initiative. T. G. gratefully acknowledges financial support of the Deutsche Telekom Stiftung, the Karlsruhe House of Young Scientists (KHYS) and the Karlsruhe School of Optics and Photonics (KSOP). M. B. C. is financially supported by the Danish Research Council for Technology and Production Sciences (Grant No. 274-09-0105). The partial support of the EC funded project NaPANIL (Contract No. NMP2-LA-2008-214249) is gratefully acknowledged. We acknowledge support by Deutsche Forschungsgemeinschaft and Open Access Publishing Fund of Karlsruhe Institute of Technology.